9 Geochemistry of Lakes

9.1 Geology of the catchment determines the composition of major ions

The chemical composition of the water and sediments of freshwater lakes reflects the geology of their catchment, anthropogenic activities, and over-regional atmospheric deposition. The density of the water may differ depending on whether its tributaries drain crystalline or calcareous catchment rocks (Table 1). As an example, such differences in the composition of major ions have significant effects e.g. on the internal flow pattern of Lake Lucerne.

Table 1: *Chemical analyses of monthly samples from Sarner Aa (tributary to Lake Alpnach, 1998/99) and Reuss at Seedorf, Canton of Uri (main tributary to Lake Lucerne from the south, aver. 2000-11).*

	Conductivity µS/cm (20°C)	**Alk** mmol/L	**Ca** mmol/L	**Mg** µmol/L	**SO_4^{2-}** µmol/L	**Si** mg/L	**pH**
Sarner Aa:	224±40	2.42±0.40	1.14±0.18	91±43	140±49	3.4±1.3	8.16±0.14
Reuss (Seedorf):	90	1.29	0.68	91	96	2.1	8.0

Lake Lucerne is divided by sills into four major and two minor basins. During winter, differential vertical mixing due to non-uniform wind exposure and different total dissolved solid concentrations in the main tributaries of the lake cause considerable inter-basin density gradients. These gradients induce density-driven currents across the sills that contribute significantly to the deep-water exchange in the basins and gradually reduce the density gradients during summer (Figure 1). Wüest et al. (1988) postulated the existence of a density-driven current from Gersauerbecken into the deep layers of Urnersee (i.e. against the main flow direction in the lake). Because of its large conductivity, water from Lake Alpnach can easily be traced in Vitznauerbecken.

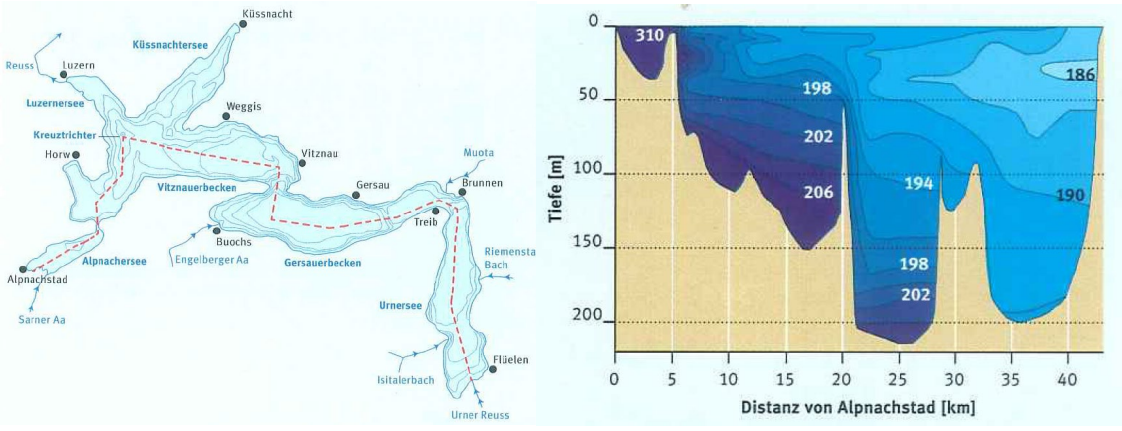

Figure 1:
Density driven exchange between the basins of Lake Lucerne (Aeschbach-Hertig et al., 1996). Numbers signify electrical conductivity (κ_{20}) in µS/cm.

9.2 Anthropogenic contributions: e.g. land use and atmospheric deposition

Atmospheric transport and deposition has become the dominant process for N contamination of ecosystems. While the natural background is estimated at ~0.5 kgN $ha^{-1}yr^{-1}$, atmospheric deposition rates on the Swiss Plateau today exceed 40 kgN $ha^{-1}yr^{-1}$ in many areas and are among the highest in the world (Figure 2, BAfU, 2010). It is one of the main environmental goals of the EU to reduce the release of N to surface waters and the atmosphere.

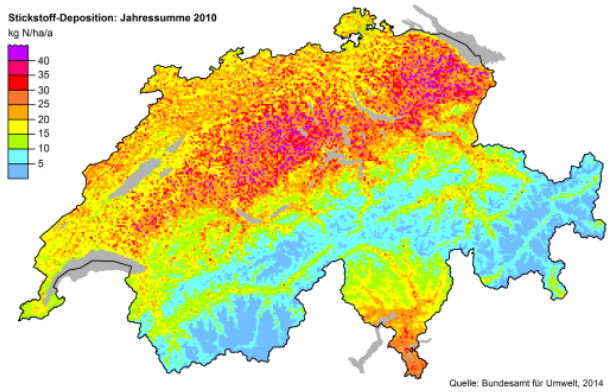

Figure 2:
Atmospheric deposition of nitrogen in Switzerland in kgN $ha^{-1}yr^{-1}$ (BAfU, 2010).

Land use and atmospheric deposition significantly imprint their emissions in the water composition of rivers and lakes, which becomes obvious in a study comprising 68 small to mid-sized lakes distributed over an altitudinal gradient in Switzerland. Striking differences in the water compositions of lakes above and below ~700 m of altitude were observed (Figure 3). Concentrations of total nitrogen and nitrate, total phosphorus, dissolve organic carbon (DOC), Na, K, Mg, Ca, and alkalinity are distinctly higher in most lakes below 700 m than above, and the pH of the bottom waters of these lakes is generally lower. Estimates of total nitrogen concentrations, even in remote areas, indicate that precipitation is responsible for increased background concentrations. At lower altitudes, nitrogen concentrations in lakes are explained by the intense agricultural land-use. In Switzerland, a maximum annual application to fields of 315 kgN $ha^{-1}yr^{-1}$ is allowed. Most of that amount is applied as manure.

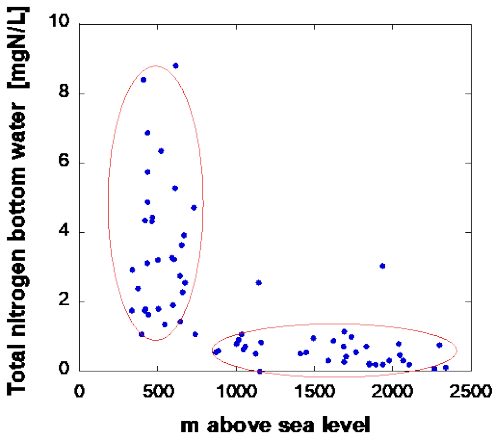

Figure 3:
Bottom water concentrations of total nitrogen in 68 small Swiss lakes (Müller et al., 1998).

9.3 Carbon cycling in lakes – an overview

During photosynthesis and chemosynthesis dissolved inorganic carbon (DIC) is converted into particulate organic carbon (POC). Although CO_2 and HCO_3^- are the forms of DIC usually assimilated by aquatic autotrophs, the entire pool of DIC may be depleted during assimilation because the chemical reactions among the four major DIC components (CO_2, H_2CO_3, HCO_3^- and CO_3^{2-}) are reversible and relatively rapid (Section 10.9.). Additionally, the percentages of the four major DIC components shift during photosynthesis because the pH usually increases (Section 10.4.).

Initially, DIC is transformed into POC via assimilation into the autotrophs' cells. Some organic carbon compounds can leak out of living cells or be leached from decomposing seston (the sum of all floating biotic and abiotic particles). When those compounds leave the particles and enter the water column, they become DOC. Common classes of DOC compounds include humic and fulvic acids, proteins, peptides, amino acids, other low molecular weight organic acids (e.g., formic, acetic, propionic, lactic, succinic), carbohydrates, hydrocarbons (e.g., alkanes, aromatics) and lipids.

In oxic water in the epilimnion (and usually in the metalimnion and the upper portion of the hypolimnion), some of the POC in biomass and detritus either (i) can be partially oxidized biotically or abiotically by O_2 or other oxidants and become DOC compounds in the water column, or (ii) can be completely oxidized to CO_2. Additionally, some of the DOC in the water column can be completely oxidized to CO_2, especially with the assistance of photochemical reactions. If CH_4 is produced in underlying anoxic zones and diffuses or bubbles up to the oxic zone, it can be oxidized to CO_2 by methanotrophs that use O_2 as their terminal electron acceptor. These processes return CO_2 to the DIC pool, usually altering the pH of the sediment porewater and water column (Section 10.9.) and thus the percentages of the components in the DIC pool.

Because its specific weight usually exceeds 1 kg L^{-1}, POM eventually settles out of the epilimnion. On the way down it reaches the temperature gradient that separates the epi- from the hypolimnion. The increase of water density due to the decrease in temperature slows the sinking process resulting in an accumulation of POM. The mineralization of POM in this strongly stratified zone results in a local decrease of O_2 (and possibly other electron acceptors, e.g. NO_3^-) and the release of degradation products such as NH_4^+. This is referred to as the '***metalimnetic minimum zone***'.

In the process of continued settling and degradation, POM loses C, N, P, and other biologically incorporated elements; however, either C is preferentially lost compared to N and P, or dissolved N and P are taken up from the water column. Therefore, the C:N and C:P ratios in particles ***decrease*** as depth in the water column increases. In this context, it is important to recognize that many heterotrophic bacteria are attached to particles as they consume DOC and POC, and these bacteria can constitute a significant portion of the particles that reach the sediment of lakes.

In lakes that have extensive littoral zones, aquatic macrophytes can contribute considerably to the primary productivity. When those plants age they can contribute considerable DOM and POM to the water column in the littoral zone. Moreover, the POM can either settle to the littoral sediments or be advected into the pelagic zone, where the particles can then descend into the hypolimnion along with POM that was produced in the pelagic zone. In the littoral, pelagic, and profundal zones, the POM can be leached to produce more DOM and/or at least partly decomposed to CO_2 during the remainder of the year.

Eventually, particles enter an anoxic zone, either while settling in the water column of a stratified eutrophic lake or after they are buried several mm to cm deep in the sediment of a mesotrophic or an oligotrophic lake. Because O_2 is no longer available as the terminal electron acceptor in that anoxic environment, microbes use alternate terminal electron acceptors to continue decomposing DOM and POM. Those terminal electron acceptors can include NO_3^-, Mn(IV), Fe(III), SO_4^{2-}, and CO_2, in the order of their decreasing favorability for net energy gain (Section 10.7.). Above the zone dominated by

methanogenesis, upward-diffusing CH_4 can be oxidized to CO_2 by methanotrophs that use NO_3^- or SO_4^{2-} as their terminal electron acceptor in the anoxic zone or by methanotrophs that use O_2 as their terminal electron acceptor in the overlying oxic zone. Methane that escapes oxidation in the sediment and water column can reach the overlying air by upward diffusion through the air-water interface or by ebullition.

Usually, the pH of the hypolimnion and interstitial water in the sediment is lower than the epilimnetic pH. Therefore, $CaCO_3$ particles settling into the hypolimnion partially dissolve. The released CO_3^{2-} and HCO_3^- increase the DIC pool, in addition to the increases of DIC from oxidation of DOC and POC. As particles get buried even deeper in anoxic sediments, POC that has not yet been fully decomposed or leached to form DOC, or $CaCO_3$ particles that have not yet completely dissolved can become permanently buried.

9.4 Primary production and photosynthesis

Primary production is the *de novo* synthesis of organic matter. Secondary production by consumers (e.g., protozoa, zooplankton, and fish) and detritivores (e.g., bacteria and fungi) does not create new organic matter; it only converts one type of organic matter into another. Thus, the autotrophy of a lake is measured at the level of primary production. In (1) large, deep lakes with a littoral zone that is small compared to the total lake area and (2) large rivers, most of the primary production is due to phytoplankton or autotrophic bacterial production. On the other hand, in shallow lakes with an extended littoral zone and in streams, production of periphyton and macrophytes usually contribute most to the *de novo* synthesis of organic matter.

Primary producers assimilate N and P (and other minor essential elements like S, Ca, Na, etc.) in addition to carbon. Hence, primary production can be represented as follows for oxygenic photosynthesizers (Stumm and Morgan 1996, p. 887ff):

$$106\ CO_2 + 122\ H_2O + 16\ NO_3^- + HPO_4^{2-} + 18\ H^+ \rightarrow C_{106}H_{263}O_{110}N_{16}P + 138\ O_2 \qquad \text{(eq. 1)}$$

where $C_{106}H_{263}O_{110}N_{16}P$ is a generalized formula for organic matter in algal cells averaged from measurements of the world oceans. The reversed process is called **mineralization**. Although the stoichiometry of eq. 1 may vary from one aquatic habitat to another, it is remarkable that the summation of the sophisticated processes of the production-respiration dynamics, in which so many organisms participate, results in such generic relations. A vertical segregation of nutritional elements occurs in lakes and in the ocean. During photosynthesis, nitrogen (NO_3^- or NH_4^+) and phosphate are taken up together with carbon (CO_2 or HCO_3^-) in the proportion 106 : 16 : 1. This is called the '**Redfield ratio**'. As a consequence of respiration (oxidation) of these organism-produced aquatic particles after settling, these elements are released again in approximately the same proportions. Respiration is accompanied by a respiration quotient $\Delta O_2/\Delta C \simeq -1.3$ (or $\Delta O_2/\Delta N \simeq -9$). It has to be noted, however, that this ratio in freshwater lakes can deviate significantly from the classic Redfield ratio (which was determined for open oceans), according to the nutrient situation and can also vary with the seasons. We have determined C:P ratios in sediment trap material of around 80 in lakes with high TP concentrations that increased, however, up to around 250 in oligotrophic lakes (Figure 4, Müller et al., 2019). Obviously, some phytoplankton species and bacteria can store P ('luxury consumption') in higher trophic systems resulting in low C:P ratios. In an oligotrophic lake, however, the phytoplankton community can adjust its requirement for P tremendously and can optimize its production of biomass.

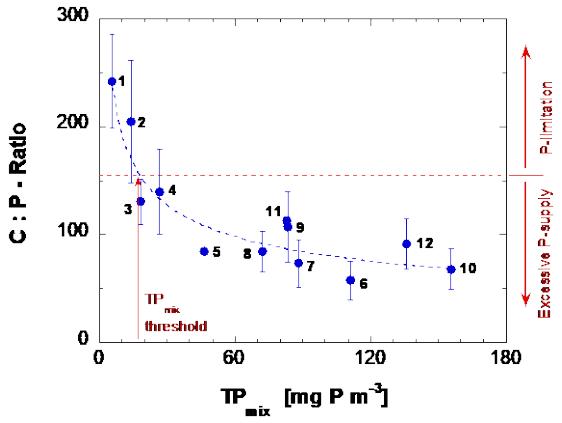

Figure 4: Molar ratios of C:P observed from settled material collected in sediment traps. *Eight European lakes with widely varying TP_{mix} concentrations were sampled and monitored over different time periods. 1: Lake Aegeri (2013-2014); 2: Lake Hallwil (2014-2016); 3: Lake Baldegg (2013-2014); 4: Lake Lucerne (1969); 5: Lake Zürich (1989); 6: Lake Zürich (1984); 7: Lake Sempach (1988-1993); 8: Lake Baldegg (1994-1996); 9: Greifensee (2002-2003); 10: Greifensee (1989-1990); 11: Lake Constance (1981-1982); 12: Lake Sempach (1984-1987).*

Hence, photosynthetic production is controlled by P as the limiting factor only over a limited concentration range. Above, photosynthesis may be limited due to 'self-shading', and no further increase of phytoplankton growth is possible even when P concentration increased further. In oligotrophic lakes, reduced production rates may occur at the surface due to transient nutrient depletion or transient photosynthetic inhibition due to high UV radiation. Most often, maximum phytoplankton growth occurs several (2 - 4) meters below the lake surface (Figure 5).

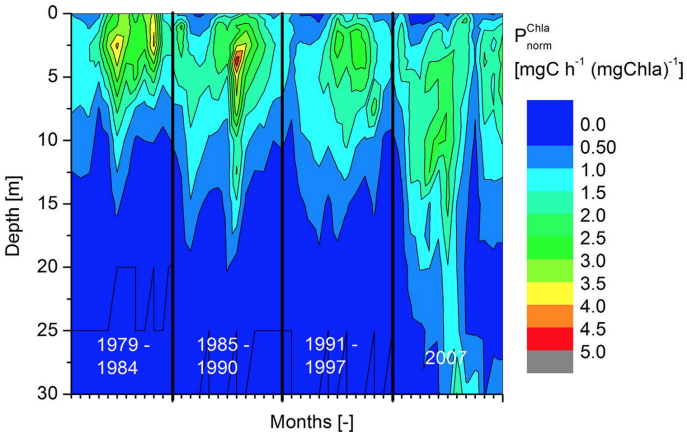

Figure 5:

Chlorophyll a concentrations in Lake Lucerne. The lake turned from mesotrophic (30 mgP m^{-3}) to oligotrophic (6.4 mgP m^{-3}) thus allowing the light to penetrate to deeper depths (Finger et al., 2013). Production maxima occur at 2 - 4 m below the lake surface.

The basic processes of assimilation, settling of particulate matter, and mineralization bring about the characteristic concentration profiles of nutrients in eutrophic lakes (Figure 6).

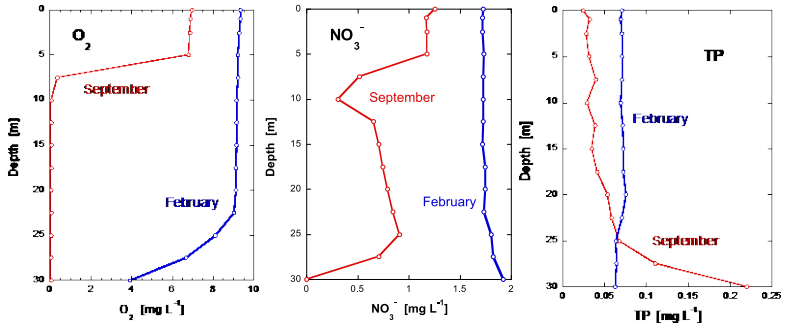

Figure 6: *Depth profiles in Greifensee: O_2, NO_3^-, and TP, February (blue) and September 2008 (red).*

10.5 Net export from the epilimnion and gross sedimentation

A large fraction of the assimilated carbon is mineralized and recycled within the epilimnion. Only 20-30% of the primary production is exported to the hypolimnion (net ecosystem production, net export production). There is no clear relationship of the exported fraction and the concentration of total P.

Gross sedimentation is the flux of carbon that eventually reaches the sediment surface and is in the order of 40-120 gC m^{-2} a^{-1}. Sediment trap data of 9 years from Lake Sempach show a range of 73±28 gC m^{-2} a^{-1}, or 38%, within this lake only (Table 2).

Table 2: *Sediment trap data (1984 – 1992) from Lake Sempach (87 m max. depth).*

Flux rate	**depth**	
[g m^{-2} a^{-1}]	20 m	81 m
Total particles	700 ± 210	770 ± 220
Carbon	61 ± 25	73 ± 28
Nitrogen	9.4 ± 3.7	12.3 ± 3.8
Phosphorus	2.0 ± 0.6	3.0 ± 0.5
Calcium	134 ± 44	126 ± 44

In lakes with depths <100m no significant loss of organic carbon is observed in the hypolimnion. Contrary, an increase is measured between sediment trap material below the epilimnion and above the lake bottom, which may be caused by bacterial growth as many heterotrophic bacteria are attached to particles as they consume DOC and POC, and these bacteria constitute a significant portion of the particles that reach the sediment of lakes. Sediment focusing may be an issue as well: Settled particulate matter can be re-suspended by water currents from steep walls and transported to deeper locations. This leads to higher sedimentation rates towards the center of the lake. E.g., in Lake Baldegg sedimentation rates are two times higher at the center than at intermediate depths.

9.6 Net sedimentation

The top few cm of the sediment is a bacterial mat with very high conversion rates. Settling organic matter drives early diagenetic processes within a thin vertically structured zone quite heterogeneous due to bioturbation by bottom dwelling organisms, differently sized particles or microzones caused by differences in composition and density of particles. With a nine year average gross sedimentation of 73 gC m^{-2} a^{-1} and a 100-year net sedimentation (expressed as mass accumulation rate) of 26 g$Cm^{-2}a^{-1}$ in Lake Sempach we estimate that about two thirds of the settling material is mineralized and one third is buried in the sediment.

An important issue for lake management is the maximum retention of phosphorus in the sediment. It is well known that some lake sediments release phosphorus when they become anoxic, which is always the case when lakes are eutrophied. In the natural environment, it appears that lake sediments have a surprisingly constant binding capacity for phosphorus. The TP net sedimentation rate increases in proportion to the ratio of catchment area to lake area (the environment factor f_U, Figure 7). This signifies that all P deposited in excess of this value can potentially be remobilized and may return to the lake water and thus to the biological cycle.

Lake Aegeri
Lake Baldegg
Lake Brienz
Lake Constance
Lake Geneva
Greifensee
Lake Hallwil
Lac de Joux
Lago Maggiore
Lake Murten
Lake Neuenburg
Pfäffikersee
Lake Sempach
Lake Thun
Türlersee
Walensee
Lake Zug
Lake Zürich

Lake Arendsee
Lake Tahoe
Lake Mendota
Lake Washington
Lake Superior
Lake Ontario
Lake Michigan
Lake Onondaga
Lake Huron
Lake Erie
Lake Biwa
Lake Qinghai
Lake Tai
Lake Chao
Lake Hongfeng
Lake Dianchi
Lake Longgan
Lake Ngoring
Lake Erhai
Lake Wuliangsu

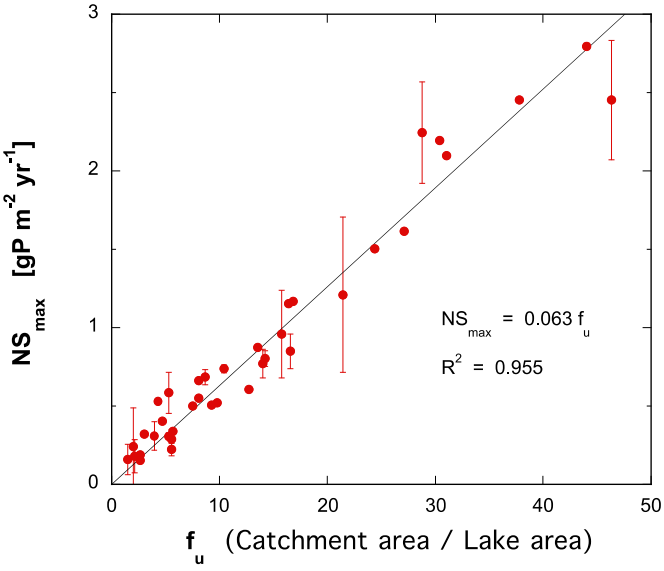

Figure 7: *Net sedimentation rates of total phosphorus (TP) at times before major human influence (at least <1940) is related to the ratio of catchment-to-lake area (f_U).*

9.7 Respiration and mineralization of organic matter

Respiration allows organisms to access energy stored in organic-chemical bonds. In *aerobic respiration*, O_2 is used to metabolize organic compounds such as carbohydrates; in *anaerobic respiration*, compounds other than O_2 are used to tap into the energy stored in carbohydrates.

E_H [V]

O_2	→	H_2O	Respiration
NO_3^-	→	N_2	Denitrification
Mn(IV)	→	Mn(II)	Mn-Reduction
NO_3^-	→	NH_4^+	Nitrate reduction
Fe(III)	→	Fe(II)	Fe-reduction
SO_4^{2-}	→	S(-II)	Sulfate reduction
CO_2	→	CH_4	Methane formation
H^+	→	H_2	Hydrogen formation
CO_2	→	CH_2O	Photosynthesis

In principle, those reactions that deliver the maximum possible energy gain are preferred (i.e. O_2 (top line) is first used up in oxidizing organic material (CH_2O, last line). The next oxidant is nitrate, followed by Mn(IV), Fe(III), SO_4^{2-}, etc. For kinetic reasons or other inhibitions (diffusion, complexation, sorption) this sequence may be confounded, however. For explicit mineralization processes, see Table 3.

9.8 Early sediment diagenesis

Concentration gradients of oxidants as well as reduced compounds in the sediment porewater indicate early diagenetic mineralization processes most sensitively (Figure 8).

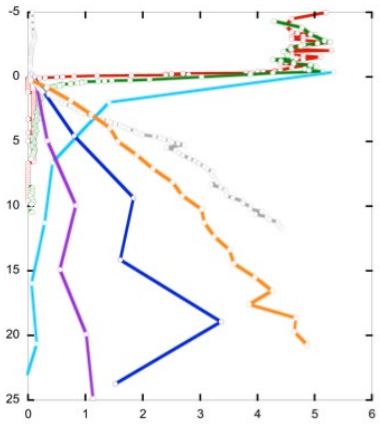

Figure 8:

Porewater concentration profiles in the top 25 mm of Lake Baldegg sediment: O_2 (red), NO_3^- (green) SO_4^{2-} (light blue), Fe(II) (blue), Mn(II) (brown), NH_4^+ (grey), CH_4 (orange).

Two processes shape the course of the porewater concentrations: (i) biogeochemical ***reactions*** in the sediment, and (ii) ***diffusion*** within the porewater. ***Reactions*** include oxidation/reduction, precipitation/ dissolution, adsorption/desorption, complexation, microbial degradation of organic material etc. ***Diffusion*** of ions in the sediment is similar to that in pure water except that it is hindered by the **porosity** (the relative porewater volume) and the **tortuosity** (the ratio of the distance that a molecule travels from A to B vs. the direct way from A to B) of the sediment (Figure 9).

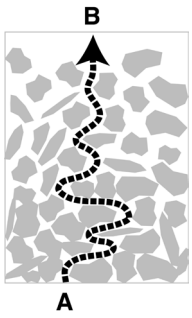

Figure 9:

Porosity and tortuosity of the sediment.

The concentration gradients in the sediment porewater are proportional to transport processes (fluxes, moles $m^{-2}\,d^{-1}$), which can be quantified with Fick's first law of diffusion, adapted to sediments:

$$J_s = -\phi D_s \frac{\partial C}{\partial x} \qquad \text{(eq. 2)}$$

where J_s is the flux of the compound in [mol $m^{-2}\,d^{-1}$], ϕ is the porosity [-], D_s the molecular diffusion coefficient in the sediment [$m^2\,d^{-1}$] (that includes the effects of tortuosity – for details see Maerki et al., 2004), C is the concentration of the compound [mol m^{-3}], and x the vertical distance [m]. Hence, a negative flux is directed to the sediment depth whereas a positive flux is directed upwards. Figure 10 shows the concentration gradient of oxygen in the sediment of Lake Alpnach after winter overturn in March when O_2 consumption is low.

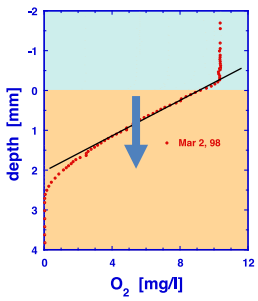

Figure 10:

Oxygen porewater concentration gradient in Lake Alpnach, 2. March 1998.

9.9 Biogenic precipitation of calcite

In the oceans, enormous blooms of the coccolithophorid emiliana huxleyi that build their shells (Figure 11, left) from calcite, cause transport of calcite to the sediments. These events are so gigantic that they can be observed by satellites (Figure 11). These organisms require water supersaturated with respect to calcite that they can build their shells.

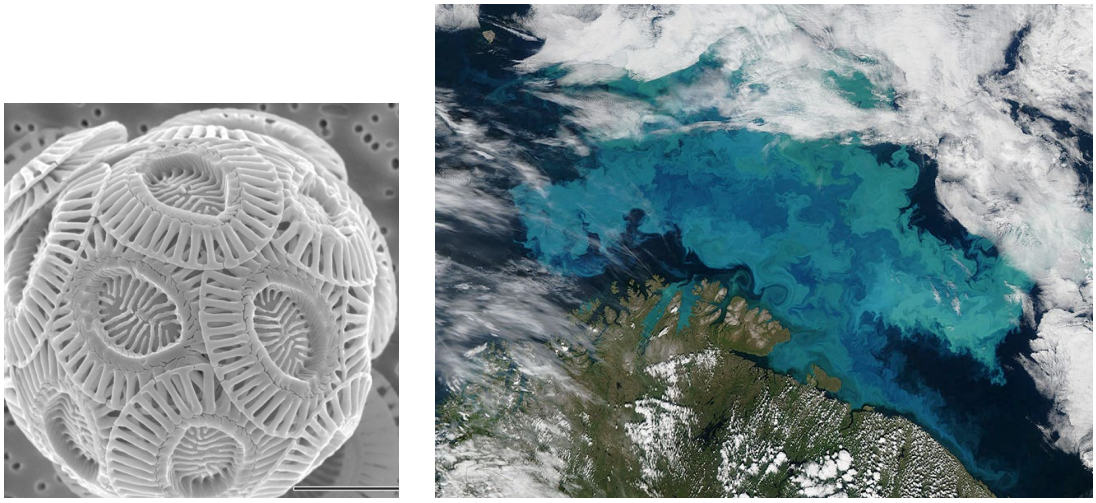

Figure 11: *Left: Calcite shell of the coccolithophorid Emiliana Huxleyi, ~10 µm. Right: Coccolithophore bloom in the Barents Sea.*

In hard-water lakes, biogenically-induced precipitation of calcite ($CaCO_3$) is the major process driving loss of alkalinity from the epilimnion. It is a well-known seasonal phenomenon caused by

i. photosynthetic assimilation of CO_2. Phytoplankton (and/or macrophytes) remove CO_2 or HCO_3^- by photosynthetic assimilation and, thus, increase the pH of the water. Calcite becomes increasingly supersaturated and eventually precipitates.
ii. surface water warming during summer stratification. The solubility of calcite decreases as temperature increases – the reverse of the solubility of most other salts.

This causes enormous annual 'whitening events' (calcite precipitation) e.g. in **Lake Michigan** (Fig. 12) or Lake Geneva (Fig. 13).

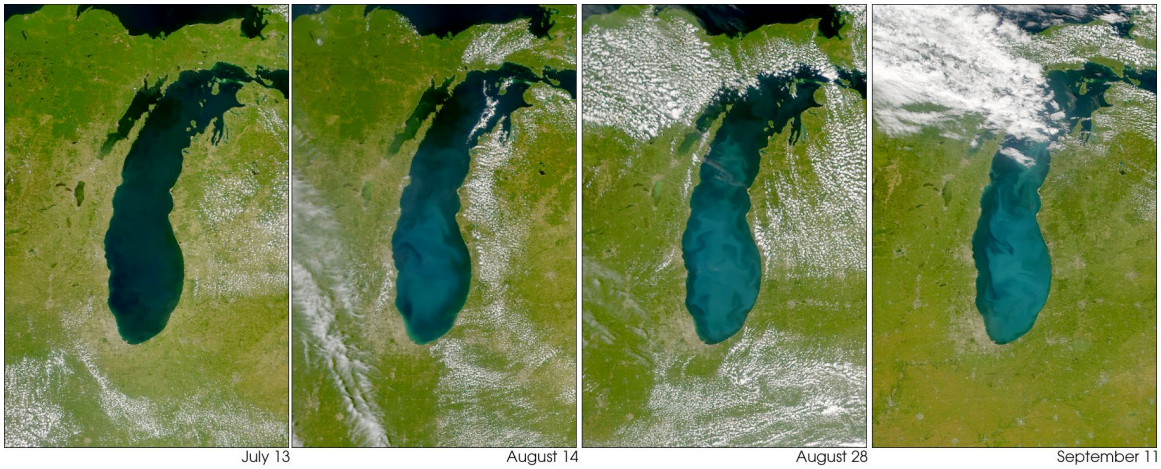

Figure 12: *Annual calcite precipitation ('whitening event') in Lake Michigan*

The whitening event in **Lake Geneva** documented by remote sensing images and chemical water data occurred on June 15, 2014 (Nouchi et al., 2019). The wide public attention to this whitening event suggests that something extraordinary may have happened in Lake Geneva in summer 2014. Actually, this was not the case. Monitoring data from 2011 to 2017 shows that the 2014 summer was quite typical.

Measurements from the water column of Lake Geneva were available in 2014 from June 2 and 30, while the event occurred close to June 16. In the top 20 m, calcite was up to five-fold supersaturated on June 2 (left panel of Figure 14). Calcite supersaturation can persist up to very high values of saturation index (Ω) without precipitation occurring for various reasons, e.g. prevention of the growth of initial nuclei by sorption of phosphate, but can be initiated by the introduction of additional nucleation seeds. It is very likely that the high particle load of the Rhône River provided such active particulate surfaces that acted as nuclei-initiating calcite precipitation, even though the river water itself was slightly below saturation with respect to calcite (saturation index Ω = 0.93). The concentrations of Ca in the top 20 m of the water column decreased between June 2 and 30 (right panel of Figure 14), indicating the removal of calcite. Integration of the Ca removed from the top 20 m yields an event-specific areal precipitation of 44 g Ca m^{-2} (1.1 mol m^{-2}).

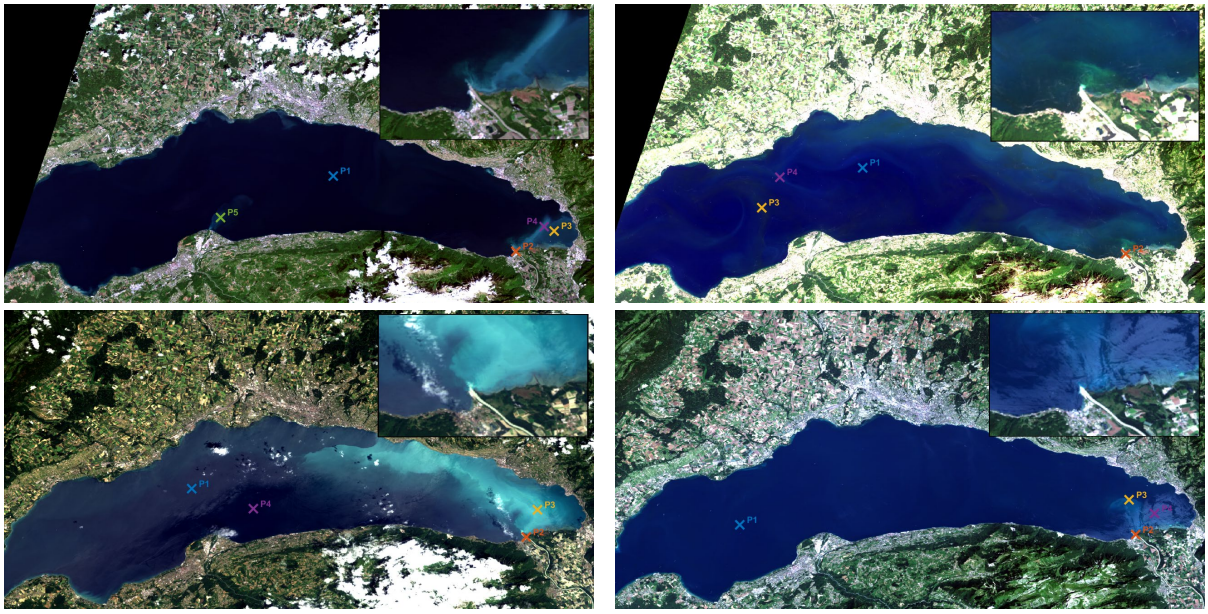

Figure 13: *Landsat-8 images of Lake Geneva from May 23 (top left), June 8 (top right), June 15 (bottom left), and July 17 (bottom right), 2014. The inset zoom shows the Rhône inflow area. Crosses indicate the pixels where water reflectance spectra were collected.*

This amount of Ca precipitation for an individual whitening event is quite realistic. In the last two decades, annual averages of Ca sedimentation in Lake Geneva were estimated to ~140 g Ca m^{-2} yr^{-1} and ~190 g Ca m^{-2} yr^{-1}, which covers a range consistent with Ca sedimentation of ~170 g Ca m^{-2} yr^{-1} as determined in the two hard-water Lakes Lugano and Sempach. This comparison indicates that this individual whitening event was removing ~¼ of an annual Ca deposition, which appears realistic in view that the Ca sedimentation was shown to scale with the organic matter production and sedimentation.

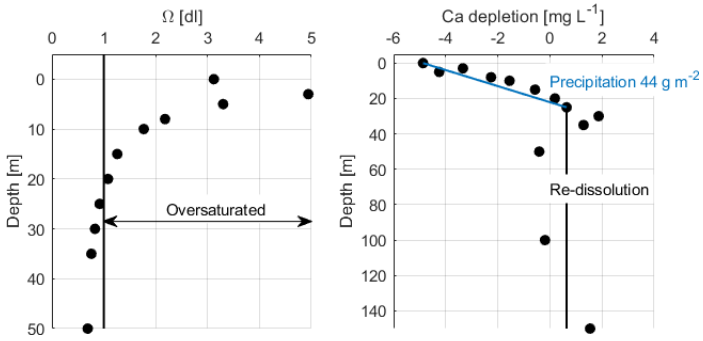

Figure 14:
Ω at SHL2 for June 2nd 2014 (left), and Ca precipitation (right) estimated over the month of June 2014 plotted as the difference in the Ca concentration between June 30th and June 2nd. The Ca depletion is restricted to the top 20 m with the maximum right at the surface. The integrated Ca precipitation for this event was 44 g m^{-2} in the top 20 m.

If the water does not maintain equilibrium with the air - often due to slow gas exchange with the atmosphere or slow diffusive transport in a poorly mixed water column, **photosynthesis** increases the pH and decreases the DIC due to a net consumption of H^+ and HCO_3^- (eq. 1). Uptake of CO_2 also consumes H^+, even though it is not immediately apparent from Equation 1. This happens because, in a "closed" system (i.e., no import or export of matter from the system), some of the CO_2 removed by photosynthesis is replaced by CO_2 generated from the dehydration of H_2CO_3* when the CO_2-H_2CO_3*-HCO_3^--CO_3^{2-} system re-equilibrates (see eq. 3 below). Thus, H^+ is consumed when HCO_3^- combines with H^+ to replace some of the H_2CO_3* (eq. 4) and when CO_3^{2-} combines with H^+ to replace some of that HCO_3^- (eq. 5). Unless nocturnal respiration in the epilimnion of a "closed" system replaces the CO_2 that is photosynthetically consumed during daylight periods, the pH of the epilimnion gradually increases and [DIC] decreases. Note, however, that alkalinity does not decrease when [DIC] decreases during photosynthetic uptake of CO_2 or HCO_3^-, because the equimolar decrease in $[H^+]$ exactly balances the uptake of DIC - leaving alkalinity unchanged. Eventually, however, the solubility product for calcite (eq. 6) will be exceeded and calcite precipitates (and, consequently, alkalinity decreases).

$CO_2(g) + H_2O$	$\Leftrightarrow$	H_2CO_3*	K_H	(eq. 3)
H_2CO_3*	$\Leftrightarrow$	$HCO_3^- + H^+$	K_{a1}	(eq. 4)
HCO_3^-	$\Leftrightarrow$	$CO_3^{2-} + H^+$	K_{a2}	(eq. 5)
$CaCO_3$ (calcite)	$\Leftrightarrow$	$Ca^{2+} + CO_3^{2-}$	K_{s0}	(eq. 6)

In the epilimnion of a productive lake, pH can increase because of a high photosynthetic rate during the daylight hours and then decrease because of a high respiration rate at night. Although diel epilimnetic pH fluctuations usually are small (<1 pH unit), they can be large in eutrophic, warm-water lakes (up to 4 pH units). This poses a challenge for researchers to decide when and where to measure lake water pH. High variability driven by alternating high photosynthesis and respiration rates can make it difficult to detect pH trends in regional studies where lakes are only sampled a few times per year.

If the pH decreases during **respiration**, $[CO_3^{2-}]$ also decreases - even though [DIC] increases when CO_2 or HCO_3^- is concomitantly produced. This process is exactly the reverse of the $[CO_3^{2-}]$ increase when pH increases during photosynthesis. In fact, $[CO_3^{2-}]$ can decrease to the point that $[Ca^{2+}]\cdot[CO_3^{2-}]$ is less than K_{s0}. Thus, respiration can cause $CaCO_3$ dissolution - a common feature in the hypolimnion of alkaline, hard-water lakes during summer stratification - as follows:

$$CaCO_3\text{ (calcite)} + CO_2(g) + H_2O \rightarrow Ca^{2+} + 2\,HCO_3^- \quad \text{or, equivalently:}$$

$$CaCO_3\text{ (calcite)} + H^+ + HCO_3^- \rightarrow Ca^{2+} + 2\,HCO_3^- \quad \text{(eq. 7)}$$

When $CaCO_3$ dissolves, alkalinity increases. Thus, respiration can indirectly increase the alkalinity of the water. However, that generally only occurs in intermediate- to hard-water, alkaline lakes in which $CaCO_3$ crystals exist in the sediments or are suspended in the water column. Dissolution of $CaCO_3$ tends to attenuate (i.e., buffer) the pH decrease resulting from respiration.

Chemical equilibrium in the water column alone does not appear to control calcite precipitation, because Ca^{2+} and CO_3^{2-} usually are present at concentrations exceeding $CaCO_3$ solubility. Instead, there are strong indications that cyanobacterial picoplankton play a key role in calcite precipitation (Obst et al., 2009). During CO_2 assimilation, cell surfaces provide (i) micro-zones of high pH within the diffusive boundary layer (DBL) surrounding the cells, and thus (ii) sites for the initiation of heterogeneous nucleation of calcite.

Niessen and Sturm (1987) observed in the historical record of the sediments in Lake Baldegg in central Switzerland, that increasing eutrophication in the 1900s led not only to more calcite precipitation but also to a ~10-fold increase in the size of calcite crystals (Figure 15). According to Kunz (1984), crystal size and $\Omega_{calcite}$ are linearly related. Furthermore, orthophosphate (i.e., $H_2PO_4^-$, HPO_4^{2-}, and PO_4^{3-}) inhibits the growth of calcite nuclei. Therefore, calcite precipitation starts at higher degrees of supersaturation and thus produces larger crystals in eutrophic than in oligotrophic lakes. Because of this, the size of autochthonously formed calcite crystals in sediments might be an indicator of changes in orthophosphate concentration and, thus, changes in trophic state of a lake.

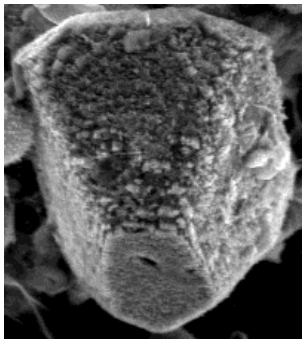

Figure 15:

Calcite crystal from the sediments of Lake Baldegg with a diameter of about 30 µm.

Biogenic precipitation of calcite as observed in Lakes Baldegg and Sempach

A unique set of data exists from these two lakes that include data from sediment traps over several years with high temporal resolution, and monthly monitoring data of all relevant parameters. The data show that calcite precipitation (green lines in Figures a and d) was restricted to several distinctly separated periods during summer stratification (Figures 16 a, d), as previously reported for Lakes Constance (Stabel, 1985) and Lucerne (Bloesch, 1974). Unlike TP (red lines in Figures a and d), epilimnetic alkalinity (blue lines) did not decrease immediately after winter circulation (March to April) in the top 10 m but instead continued to increase until May or even June or July, when calcite precipitation started. Thereafter, epilimnetic TP concentration and alkalinity decreased concurrently and rapidly, indicating a coupled transformation of bicarbonate/carbonate and phosphorus from the dissolved to the particulate phase and subsequent settling of calcite and phosphorus as described by Sturm et al. (1982). Epilimnetic alkalinity started to decrease when the surface saturation index Ω_{CO2} approached or fell below unity (compare Figure 16a with 16b and Figure 16d with 16e).

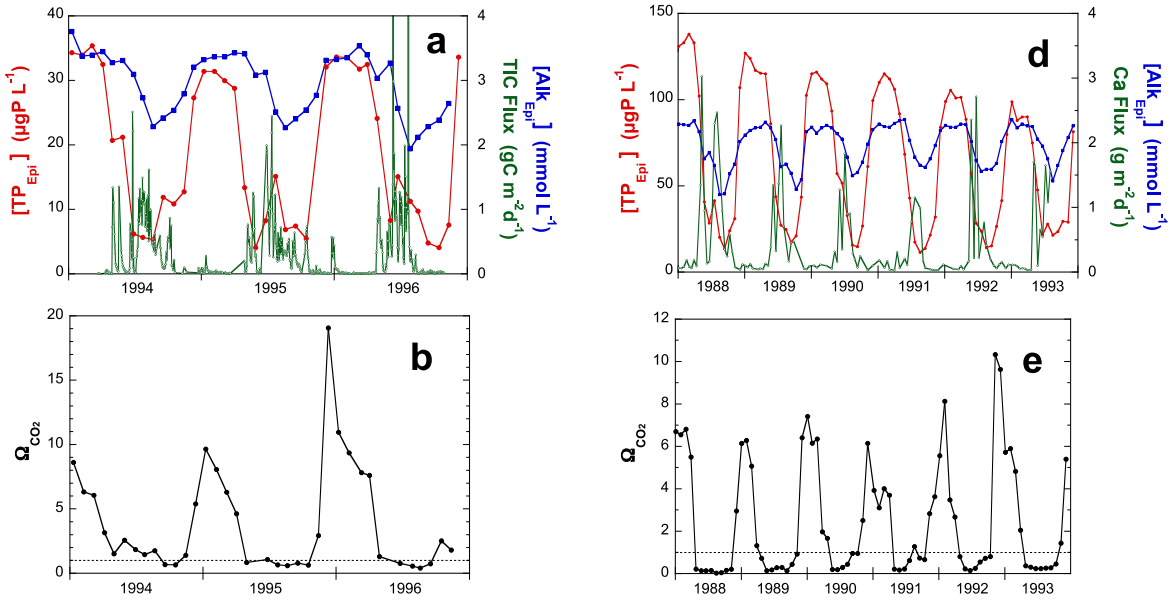

Figure 16:
Monthly data of a-b) Lake Baldegg and d-e) Lake Sempach. a) and d): seasonal variation of $CaCO_3$ settling flux from sediment traps (green curves: TIC flux in (a) Lake Baldegg (M. Sturm, unpublished data), Ca^{2+} flux in (d) Lake Sempach (Gächter and Meyer, 1990)), epilimnetic alkalinity ([Alk_{epi}]; blue curves), and epilimnetic total phosphorus concentration ([TP_{epi}]; red curves). b) and e): surface-water CO_2 saturation index (Ω_{CO2}; =[CO_2(aq)]/[CO_2(atm)]). (Müller et al., 2016).

Hard-water lakes are sources of CO_2 to the atmosphere

Lakes situated in calcareous catchments are sinks for calcite. Net CO_2 production by heterotrophic soil organisms results in elevated concentrations of carbonic acid in the water percolating through the soil, dissolving calcite and thus elevating concentrations of Ca^{2+}, HCO_3^-, and CO_3^{2-}. Consequently, newly-emerging groundwater is super-saturated with respect to CO_2 and calcite. Some of the Ca^{2+} and CO_3^{2-} precipitate to form calcite as the CO_2 concentration equilibrates with the atmosphere (resulting in higher pH). As Figures 16b and 16e show, lakes vent excess CO_2 during and immediately after spring overturn. This excess CO_2 originates from (i) CO_2 that accumulated in the hypolimnion due to microbial decomposition of organic matter, (ii) direct infiltration of CO_2-super-saturated groundwater into the hypolimnion (Lewandowski et al., 2014), and (iii) tributaries importing water that had not equilibrated with the atmosphere before reaching the lakes (Gruber et al., 2000; Marcé et al., 2015). Therefore, lakes with alkalinity exceeding approximately 1.2 mmol L^{-1} are sources of CO_2 to the atmosphere during spring overturn (Müller et al., 2016).

9.10 The concept of alkalinity

The alkalinity of calcium carbonate-saturated lakes is generally defined as the capacity to neutralize acid. Hence it is the sum of bases (compounds that can take up protons) minus the sum of acids (compounds that can release protons):

$$Alk = [HCO_3^-] + 2[CO_3^{2-}] + [OH^-] - [H^+] \qquad \text{(eq. 8)}$$

Most often in carbonate-buffered waters all other acids and bases are negligible compared to carbonate, hence they do not need mentioning in eq. 8. This concept requires reference states of all acid-base-pairs involved, which in this case is the fully protonated carbonic acid, H_2CO_3, and H_2O. For a more profound view of the alkalinity concept see Stumm and Morgan (1996, p. 163ff).

What makes alkalinity as a chemical parameter so important? Initially, it is difficult to comprehend what this construct can be useful for. However, it has several great inherent properties:

- Alkalinity can be determined with a simple acid-base titration and is expressed as a concentration (eg. mmol L^{-1}).
- Alkalinity is a conservative chemical parameter, i.e. it is independent of temperature and pressure, although individual species such as pH and H_2CO_3 are not.
- Alkalinity does not change when one of the reference compounds (H_2CO_3, or CO_2 in this case) change or when other substances change that do not appear in eq. 8 and are neither acids nor bases are added to or removed from the system.
- Many redox processes consume (oxidations) or produce (reductions) alkalinity, hence the change of alkalinity in either time or space is an invaluable parameter to conclude on processes and estimate reaction rates.

In any investigation of the inorganic carbon system in natural waters, alkalinity is a great help. While the concentration of CO_2, and thus the concentration of total inorganic carbon, changes quickly when the partial pressure of CO_2 (p_{CO2}) changes [eg. a water sample is retrieved from the lake where at certain depths CO_2 is consumed (by photosynthesis) or produced (by mineralization)] or when the water temperature changes, alkalinity remains unaltered. Hence, the sample can be transported to the lab and analyzed without great precautions and conservation. The pH, an essential parameter to calculate chemical equilibria, changes with temperature and pressure, however, *in situ* measurements are simple and generally integrated in profiling probes. Alkalinity in combination with pH then allows the simple calculation of total dissolved inorganic carbon and the concentration of CO_2 in natural waters.

Alkalinity changes during reductions and oxidations in natural waters

Alkalinity is generated when specific oxidants (O_2, NO_3^-, Fe(III), Mn(IV), …) are reduced (H^+ are consumed), and consumed when reduced species (NH_4^+, Fe(II), S(-II), …) are oxidized (H^+ are produced) (Table 3).

Table 3: *Redox reactions in natural waters and change in alkalinity. ΔAlk is given in equivalents of alkalinity per equivalent of oxidant or reductant.*

Oxidant	Process	Reaction	ΔAlk
O_2	Respiration	$C_{106}H_{263}O_{110}N_{16}P + 138O_2 = 106CO_2 + 16NO_3 + HPO_4 + 122H_2O + 18H$	-0.13
	Respiration	$C_{106}H_{263}O_{110}N_{16}P + 106O_2 + 14H = 106CO_2 + 16NH_4 + HPO_4 + 106H_2O$	0.13
NO_3	Denitrification	$(CH_2O)_{106}(NH_3)_{16}(H_3PO_4) + 84.8NO_3 + 95.8H = 106CO_2 + 16NH_4 + HPO_4 + 42.4N_2 + 148.4H_2O$	1.1
NO_2			
Mn(IV)	Mn-reduction	$(CH_2O)_{106}(NH_3)_{16}(H_3PO_4) + 212MnO_2 + 398H = 212Mn^{2+} + 16NH_4 + 106CO_2 + HPO_4 + 298H_2O$	1.9
CH_2O	Fermentation	$3CH_2O + H_2O = CO_2 + 2CH_3OH$	0
Fe(III)	Fe-reduction	$(CH_2O)_{106}(NH_3)_{16}(H_3PO_4) + 424\ Fe(OH)_3 + 862H = 424Fe^{2+} + 16NH_4 + 106CO_2 + HPO_4 + 1166H_2O$	2.0
SO_4	Sulfate reduction	$(CH_2O)_{106}(NH_3)_{16}(H_3PO_4) + 53SO_4 + 67H = 106CO_2 + 16NH_4 + HPO_4 + 53HS + 106H_2O$	1.3
CH_2O	Methanogenesis	$2CH_2O = CH_4 + CO_2$	0

Reductant	Process	Reaction	ΔAlk
CH_4	CH_4 oxidation	$CH_4 + 2O_2 = CO_2 + 2H_2O$	0
	CH_4 oxidation	$CH_4 + SO_4 + H = CO_2 + HS + 2H_2O$	1
NH_4+	Nitrification	$NH_4 + 2O_2 = NO_3 + 2H + H_2O$	-2
Mn(II)	Mn-oxidation	$Mn(II) + 0.5O_2 + H_2O = MnO_2 + 2H$	-2
C_{org}	Oxic mineralisation	$C_{106}H_{263}O_{110}N_{16}P + 138O_2 = 106CO_2+16NO_3+HPO_4+122H_2O+18H$	-18
Fe(II)	Fe-oxidation	$Fe(II) + 3H_2O = Fe(OH)_3 + 3H + e$	-3
FeS_2	Pyrite oxidation	$FeS_2 + 3.75O_2 + 3.5H_2O = Fe(OH)_3 + 2SO_4 + 4H$	-4
H_2S	Sulfide oxidation	$H_2S + 2O_2 = SO_4 + 2H^+$	-2

9.11 Oxygen depletion in lakes

Depletion of dissolved oxygen (O_2) in the hypolimnia of lakes during stratification and its deleterious effect on fish stocks has been observed and analyzed for more than hundred years. Issues with water quality related to O_2 depletion from lake hypolimnia during the stratified season led to improved lake and reservoir management during the 1960s and 1970s. As biologically available phosphorus (P_{bio}) was recognized as the driving force for primary production, management efforts focused primarily on reducing P loads to lakes (Vollenweider, 1968; Schindler, 2006). Costly efforts on lake remediation such as advanced sewage treatment, ban of P in detergents, or reduction of diffusive nutrient loads from agriculture proved successful in preventing algal blooms and fish kills. As a result, P concentrations decreased in many lakes since the mid-1970s and early 1980s, creating a success story in water management (Hering et al., 2012), e.g. illustrated for Lakes Sempach and Baldegg in Figure 20 where the reduction of the P_{bio} load lowered the in-lake TP concentration from >500 mgP m^{-3} to <30 mgP m^{-3}.

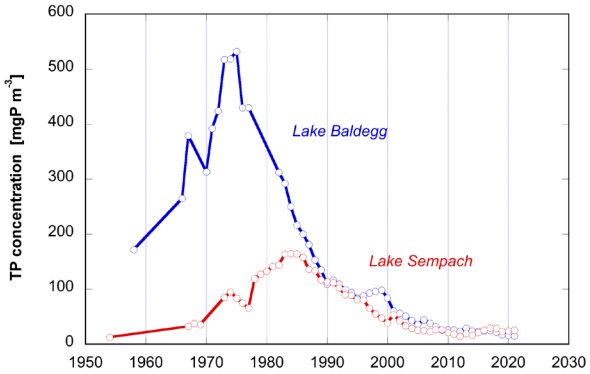

Figure 20:

Temporal development of total phosphorus concentrations after winter circulation in Lakes Sempach and Baldegg.

It was soon recognized, however, that the link between P_{bio} and hypolimnetic O_2 consumption was more complex than initially thought. On the one hand, internal lake measures such as hypolimnetic oxygenation through artificial aeration aiming at preventing the release of P from the reduced sediment did not show the expected success with respect to sediment P retention (Gächter and Wehrli, 1998). On the other hand, it was puzzling to observe that in spite of the decreasing P contents, **areal hypolimnetic mineralization** rates (**AHM**) remained tenaciously unaffected (Figure 21).

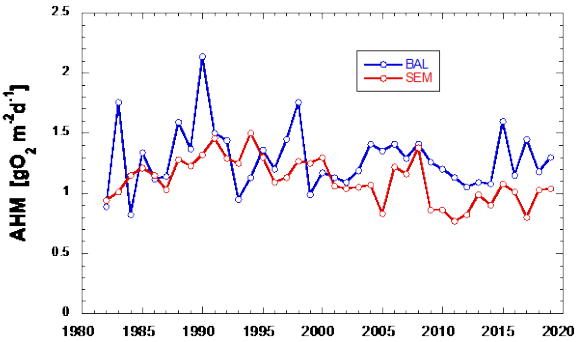

Figure 21:

No temporal trends in areal oxygen consumption rates (AHM)in Lakes Sempach (red) and Baldegg (blue) in spite of decreasing P_{bio}.

Estimation of areal hypolimnetic mineralization rates: Conceptually, AHM considers the O_2 consumed in the hypolimnion but also includes reduced compounds that prevail in the water column such as CH_4, NH_4^+, etc. (F_{red}) that diffuse from the sediment layers. Eqs. 10a to 10e summarize the key processes including the O_2 equivalents required for their oxidation.

CH_4	+	$2\ O_2$	=	$CO_2 + 2\ H_2O$	(10a)
NH_4^+	+	$2\ O_2$	=	$NO_3^- + H_2O + 2\ H^+$	(10b)
NO_2^-	+	$0.5\ O_2$	=	NO_3^-	(10c)
Mn(II)	+	$0.5\ O_2 + 2\ H^+$	=	$Mn(IV) + H_2O$	(10d)
Fe(II)	+	$0.25\ O_2 + H^+$	=	$Fe(III) + 0.5\ H_2O$	(10e)

We analysed a large monitoring datasets from 24 Swiss lakes consisting of more than 55'000 O_2 measurements and estimated annual AHM (Müller et al., 2012). A surprisingly clear picture emerged as AHM increased with mean hypolimnion depth (Figure 22). The result for eutrophic lakes (red dots) suggests two sinks for O_2: (i) the oxidation of reduced substances diffusing from deeper sediment layers, and (ii) the mineralization of freshly settled organic material at the sediment surface. The following relationship was deduced and is depicted by the red line in Figure 22:

$$AHM(z_H) = F_{red} + \frac{D_{O_2}}{\delta \times \Delta t} \int_0^{200d} C(t)dt \qquad \text{(eq. 11)}$$

Here, F_{red} = 0.3 $gO_2\ m^{-2}\ d^{-1}$ is the flux of dissolved reduced substances from the sediment porewater expressed in equivalents of O_2 required for their oxidation (intercept in Figure 22), D_{O2} is the molecular diffusion coefficient for O_2, $C(t)$ is the volume-averaged hypolimnetic O_2 concentration as a function of time, δ the thickness of the diffusive boundary layer at the sediment-water interface (fitted to the data, δ = 1.2 mm), and the integration is over the duration of the stratified period ($\Delta t \approx$ 200 days for these lakes). The initial O_2 concentration at the onset of lake stratification was set to 10.5 mg L^{-1}. This surprising correlation imposes several hypotheses valuable for eutrophic lakes:

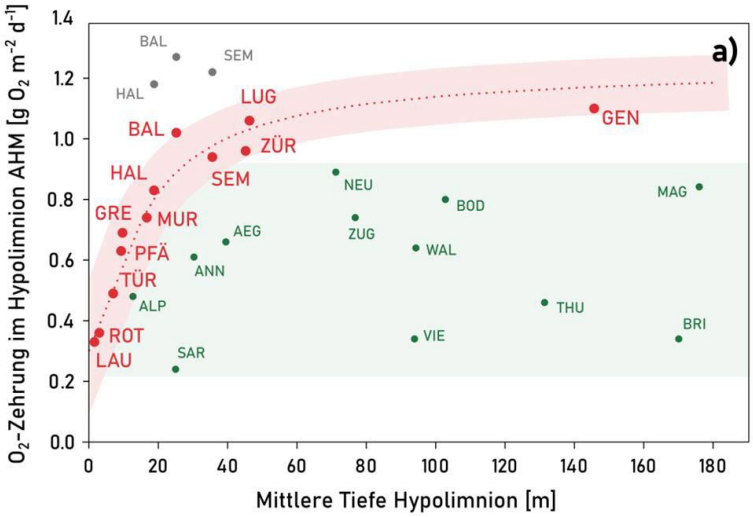

Figure 22: *Areal hypolimnetic mineralization rate (AHM) of 20 lakes as a function of mean hypolimnion depth* z_H. *For eutrophic lakes (red), AHM correlates with depth unless they are aerated (grey dots), but not for meso- to oligotrophic lakes (green).*

Maximum flux of particulate organic carbon to the sediment: Figure 22 shows that AHM asymptotically approaches an upper limit with increasing z_H of eutrophic lakes. The productive surface zone of eutrophic lakes extends only over ~15 m in the vertical direction regardless of the lake size; hence, primary production is limited to a maximum of ~400 to 500 gC m^{-2} yr^{-1}. For several eutrophic lakes, measurements of net export from the epilimnion and benthic gross sedimentation rates are available from a number of sediment-trap studies (e.g. Table 2). Maximum net export rates of carbon from the trophic zone into the hypolimnion are thus in a similar range with an upper estimate of □100 gC m^{-2} yr^{-1} despite very different P concentrations. Moreover, sediment-trap data in Table 2 also show that fluxes from bottom traps are not significantly different from those from traps directly below the epilimnion. These results are supported by sediment-trap data from Bernasconi et al. (1997) in Lake Lugano showing primary production of 300 gC m^{-2} yr^{-1} and benthic sedimentation of 109 gC m^{-2} yr^{-1}.

As expected, the AHM of the meso- to oligotrophic lakes presented in Figure 22 (green dots) did not fall on the red line. Obviously, if the O_2-storage capacity of a lake's hypolimnion is big enough, the lake is protected from becoming anoxic during summer stratification. Lake Geneva, even though highly productive, has such a large O_2 reservoir that bottom water O_2 concentrations are always high enough to allow almost complete mineralization of the settled organic matter with O_2. A substantial fraction of the O_2 consumption occurs in the water column (Schwefel et al., 2018).

In consequence, there are specific differences between shallow (<40 m deep) and deep (>40 m deep) lakes with respect to their ability to mineralize settling organic matter:

Eutrophic lakes of <40 m depth deposit more organic matter on the bottom than can be mineralized with oxygen. Oxygen consumption rates attain a maximum value that is controlled by the bottom water oxygen concentration. Excess organic matter remains in the sediment, where slower anoxic mineralization processes produce reduced compounds that diffuse from the porewater (mainly CH_4 and NH_4^+) to the lake bottom water and consume O_2 in the bottom water. **The oxygen consumption rate is controlled by the concentration of oxygen in the bottom water**. These lakes will not react immediately to a decrease in the phosphorus load due to the inherited organic matter deposition from the time of eutrophication but continue to consume oxygen at a maximum rate.

Lakes of >40 m depth, even if they are (or were) eutrophic (such as Lakes Geneva, Constance, and Zürich), and oligotrophic lakes always have (or had) plenty of oxygen in their bottom water to mineralize all settling organic matter. They bear no inherited reduced load in their sediments, and **oxygen consumption is mainly controlled by the amount of freshly settling organic matter**. Hence, as the phosphorus load is reduced below a critical limit where primary production decreases as well, the oxygen consumption rate also decreases simultaneously. Hence, oxygen consumption rates (AHM) of deep lakes show a maximum in case they are highly productive and decrease proportionately when TP decreases below a critical threshold.

Therefore, we can expect a relationship between the algae-available P in the photic zone of a lake and the mineralization rate (AHM). In Figure 23 we plotted AHM against the per-area algae-available P, APS [g P m^{-2}] (consisting of the sum of P already present in the trophic zone in spring, and the P import from the catchment during the time of stratification). The consumption rate of oligotrophic lakes is approximately proportional to the amount of available P. Above a threshold level of APS, however, the relationship with P disappears and the consumption rate attained a maximum value of 1.06 ± 0.08 g O_2 $m^{-2}d^{-1}$. The lakes marked in red show a maximum production where P is not the controlling factor. This explains why many lakes did not show a change in their bottom water O_2 consumption in spite of a significant improvement of the P load from the catchment. A decreasing AHM can only be expected when APS crosses the threshold value of ~0.54 g P m^{-2}.

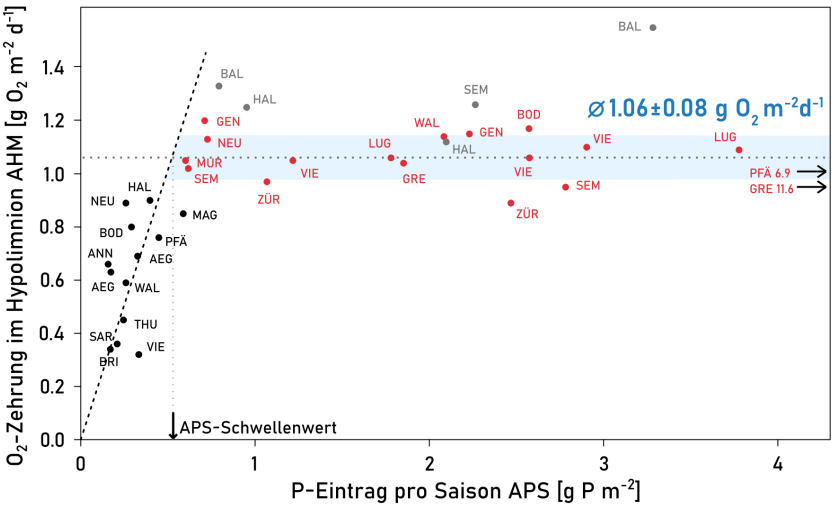

Figure 23: *AHM in deep or oligotrophic lakes: Oxygen consumption rate is maximal when lakes were eutrophic, however, the rates decrease in proportion to TP when productivity decreases. These lakes react without delay to a reduction of the TP concentration.*

The phytoplankton community can keep up their bio-production over a wide range of P concentrations. It can adjust their requirement for P to availability and adapt community composition. Macroscopically, this results in an increase of the C:P ratio of organic particulate matter as shown in Figure 24.

The transition of a lake from the state of P-saturation to a state of P-limitation was traced for Lake Hallwil, a 10 km^2 and 44 m deep lake on the Swiss plateau that reoligotrophicated from 240 mgP m^{-3} in 1979 to 11 mgP m^{-3} today (Figure 24). The C:P ratio of the phytoplankton (red line in Figure 24) indicates the dynamic adaptability. At high P availability (before 2005, phase I), the C:P ratio was ~165 while algae growth was not limited by P. The concentrations of DIP in springtime (light blue line) approached detection limits and further declines in TP concentrations forced phytoplankton to optimize P use to maintain high assimilation rates (phase II). As a consequence, the $(C:P)_{epi}$ ratio of organic particles increased, while the biomass remained roughly constant (not shown). After 2012, phytoplankton could no longer adjust C:P ratios, and further declines in P concentrations began to limit phytoplankton biomass (phase III). The $(C:P)_{epi}$ ratio reached maximum values and remained roughly

constant at ~290 (average from 2012 to 2019). The biomass began decreasing once TP_{mix} fell below a threshold TP_{mix} concentration of ~15 to ~20 mg P m^{-3} (not shown). The biomass decreased by ~50% during phase III.

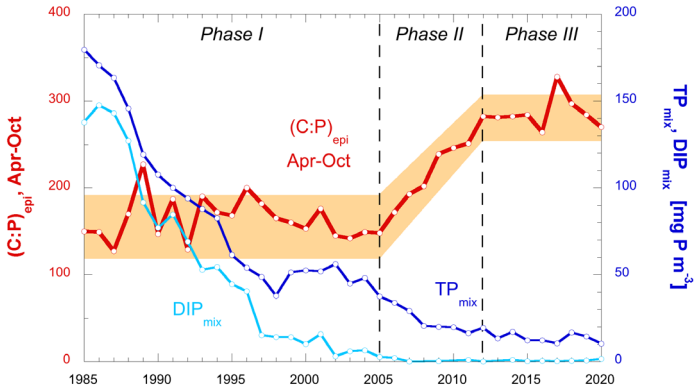

Figure 24: *$(C:P)_{epi}$ molar ratios for seston in the epilimnion (0 – 13 m depth) of Lake Hallwil averaged from April to October (red); TP_{mix} (dark blue) and DIP_{mix} (light blue) represent volume-averaged concentrations after winter overturn.*

9.12 References

Aeschbach-Hertig W., R. Kipfer, M. Hofer, DM. Imboden, H. Baur: Density-driven exchange between the basins of Lake Lucerne (Switzerland) traced with the ^{3}H-^{3}He method. Limnol. Oceanogr. 41/4, 707-721, 1996.

BAFU, 2010: Stickstoffflüsse in der Schweiz. Bafu.admin.ch/uw-1309-d. https://www.bafu.admin.ch/bafu/en/home/topics/air/state/data/historical-data/maps-of-annual-values/map-of-nitrogen-deposition.html

Bernasconi S., A. Barbieri, M. Simona. Carbon and nitrogen isotope variations in sedimenting organic matter in Lake Lugano. Limnol. Oceanogr. 42/8, 1755−1765, 1997.

Fricker H.: OECD Eutrophication Program. Regional Project 'Alpine Lakes'. 1980. BUWAL, Bern.

Gächter R., B. Wehrli. Ten years of artificial mixing and oxygenation: no effect on the internal phosphorus loading of two eutrophic lakes. Environ. Sci. Technol. 32, 3659-3665, 1998.

Gruber N., B. Wehrli, and A. Wüest. 2000. The role of biogeochemical cycling for the formation and preservation of varved sediments in Soppensee (Switzerland). J. Paleolim. 24, 277-291.

Guildford SJ., and RE. Hecky. Total nitrogen, total phosphorus and nutrient limitation in lakes and oceans: is there a common relationship? Limnol. Oceanogr. 45/6, 1213-1223, 2000.

Hering JG. E. Hoehn, A. Klinke, M. Maurer, A. Peter, P. Reichert, CT. Robinson, K. Schirmer, M. Schirmer, B. Wehrli. Moving targets, long-lived infrastructure, and increasing needs for integration and adaptation in water management: An illustration from Switzerland. Environ. Sci. Technol. 46/1, 112-118, 2012.

Lewandowski, J., K. Meinikmann, G. Nützmann, and DO. Rosenberry. 2014. Groundwater – the disregarded component in lake water and nutrient budgets. 2. Effects of groundwater on nutrients. Hydrol. Proc. 10. Doi: 10.1002/hyp.10384.

Marcé, R., B. Obrador, JA. Morgui, JL. Riera, P. Lopez, and J. Armengol. 2015. Carbonate weathering as a driver of CO_2 supersaturation in lakes. Nature geosci. Doi:10.1038/NGEO2341.

Märki M., B. Wehrli, C. Dinkel, and B. Müller: The influence of tortuosity on molecular diffusion in freshwater sediments of high porosity. Geochim. Cosmochim. Acta 68/7, 1519-1528, 2004.

Müller B., AF. Lotter, M. Sturm, A. Ammann: Influence of catchment quality and altitude on the water and sediment composition of 68 small lakes in central Europe. Aquatic Sci. 60, 316-337 (1998).

Müller B., Y. Wang, and B. Wehrli: Cycling of calcite in hard water lakes of different trophic states. Limnol. Oceanogr. 51(4), 1678-1688 (2006).

Müller B., LD. Bryant, A. Matzinger, A. Wüest Hypolimnetic oxygen depletion in eutrophic lakes. Environ. Sci. Technol. 2012a. doi 10.1021/es301422r.

Müller B., JS. Meyer, and R. Gächter. The regulation of alkalinity in calcium carbonate-buffered lakes. Limnol. Oceanogr. 61, 341-352 (2016).

Niessen, F., Sturm, M., 1987. The sediments of Lake Baldegg (Switzerland)—sedimentary environment and development of eutrophication for the last 100 yr. (in German, with English abstract). Arch. Hydrobiol. 108/3, 365–383, 1987. doi:10.4319/lo.2005.50.3.0914/pdf

Nouchi V., Kutser T., Wüest A., Müller B., Odermatt D., and Bouffard D. 2019. Resolving biogeochemical processes in lakes using remote sensing. Aquatic Sci. 81:27. doi:10.1007/s00027-019-0626-3.

Obst M., B. Wehrli, and M. Dittrich. $CaCO_3$ nucleation by cyanobacteria: laboratory evidence for a passive, surface-induced mechanism. Geobiol. 7, 324-347, 2009.

Schindler DW. Recent advances in the understanding and management of eutrophication. Limnol. Oceanogr. 51, 356-363, 2006.

Schwefel. R., Steinsberger, T., Bouffard, D., Bryant, L.D., Müller, B., and Wüest, A. Using small-scale measurements to estimate hypolimnetic oxygen depletion in a deep lake. Limnol. Oceanogr. 63, S54-S67, 2018.

Sterner RW., T. Andersen, JJ. Elser, DO. Hessen, JM. Hood, E. McCauley, and J. Urabe. Scale-dependent carbon : nitrogen : phosphorus seston stoichiometry in marine and freshwaters. Limnol. Oceanogr. 53/3, 1169-118, 2008.

Stumm, W., and JJ. Morgan. Aquatic Chemistry, Wiley Intersci., 3rd Ed. 1996.

Vollenweider RA. The scientific basis of lake eutrophication, with particular reference to phosphorus and nitrogen as eutrophication factors. Tech. Rep. DAS/DSI/68.27, OECD, Paris 1968, pp 159.

Wüest A., DM. Imboden, M. Schurter. Origin and size of hypolimnic mixing in Urnersee, the southern basin of Vierwaldstättersee (Lake Lucerne). Schweiz. Z. Hydrol. 1988, 50, 1, 41-70.